

## Article

### Effect of an Electric Field on the Growth and Optoelectronic Properties of Quasi-One-Dimensional Organic Single Crystals of 1-(Phenylazo)-2-naphthol

Chong-yang Liu, Vincent Lynch, and Allen J. Bard

*Chem. Mater.*, **1997**, 9 (4), 943-949 • DOI: 10.1021/cm9605025

Downloaded from <http://pubs.acs.org> on January 23, 2009

## More About This Article

Additional resources and features associated with this article are available within the HTML version:

- Supporting Information
- Links to the 2 articles that cite this article, as of the time of this article download
- Access to high resolution figures
- Links to articles and content related to this article
- Copyright permission to reproduce figures and/or text from this article

[View the Full Text HTML](#)



**ACS Publications**  
High quality. High impact.

# Effect of an Electric Field on the Growth and Optoelectronic Properties of Quasi-One-Dimensional Organic Single Crystals of 1-(Phenylazo)-2-naphthol

Chong-yang Liu, Vincent Lynch, and Allen J. Bard\*

Department of Chemistry and Biochemistry, The University of Texas at Austin,  
Austin, Texas 78712

Received September 26, 1996. Revised Manuscript Received February 12, 1997<sup>®</sup>

Organic single-crystal thin films (2–10  $\mu\text{m}$  thick) of 1-(phenylazo)-2-naphthol (Sudan I) were grown by capillary filling from its molten state ( $\sim 133\text{ }^\circ\text{C}$ ) into cells constructed of two parallel pieces of indium tin oxide (ITO) coated glass followed by slow cooling to room temperature. The solidified crystals were needle-shaped, a few tens of micrometers in diameter, and were aligned parallel to both ITO surfaces. Needle-shaped crystals of Sudan I were also grown from solution. X-ray diffraction analysis revealed a monoclinic crystal with space group,  $P2_1/c$  (No. 14), having  $a = 5.8225(15)$ ,  $b = 17.377(5)$ ,  $c = 24.598(5)$   $\text{\AA}$ ,  $\beta = 92.37(2)^\circ$ ,  $V = 2486.7(11)$   $\text{\AA}^3$ ,  $Z = 8$ ,  $\rho = 1.33$   $\text{g cm}^{-3}$ . The planar molecules are stacked parallel to one another to form molecular columns along the needle axis. The pattern of crystal growth can be changed by the application of an electric field between the two ITO electrodes during solidification to produce crystal needles tilted at an angle relative to the ITO surface. The electrical conductivity parallel to the crystal needle axis is over 100 times higher than that perpendicular to it due to the better  $\pi$ - $\pi$  overlap among the molecules along the needle. The electric-field-induced reorientation of the quasi-one-dimensional molecular crystals increased the conductivity of the ITO/Sudan I/ITO cells by 8–9 times. Moreover, the short-circuit photocurrent generated from these cells was enhanced by 14 times, indicating that the interfacial separation power of photon-produced electron/hole pairs was also improved substantially. This is the first example of optimization of the optoelectronic properties of molecular crystal-based devices through the manipulation of crystal orientation by an electric field.

## Introduction

In recent years, we have seen increased interest in the study of organic molecular crystals and their application in optics and electronics.<sup>1–7</sup> Much work has been done on the molecular design, synthesis, and assembly of structures with desired properties.<sup>8</sup> Although considerable progress has been made in the synthesis of different molecular structures, our understanding of how the structure and crystallographic arrangement affects the fundamental optoelectronic

properties of the organic solid is still at an early stage.<sup>9</sup> We have been particularly interested in the electrical, photovoltaic, and optoelectronic properties of symmetrical sandwich cells comprised of thin ( $\sim \mu\text{m}$ ) films of dyes and porphyrins between conductive indium tin oxide (ITO) electrodes.<sup>1,2</sup> Such cells show large differences in conductivity in the dark and under illumination. This permits charge to be injected under bias with illumination; the charge remains trapped in the dark, making these cells potential devices for information storage.<sup>1a</sup> One problem in obtaining a better understanding of the electrical properties of molecular solids is that most organic compounds can be synthesized only in the form of small crystals or polycrystalline powders, layers, or films due to relatively weak short-range intermolecular forces. Measurements from these systems often yield results that can be understood only on a qualitative level.<sup>9</sup> For example, grain boundaries have a dramatic influence on charge-carrier transport,<sup>1e</sup> and this effect can mask the intrinsic electronic nature of the conductance in organic materials. Moreover, crystal orientation significantly affects the optoelectronic properties. Such anisotropic effects, however, cannot be studied in a polycrystalline system. Another factor, not explored in this paper, is the effect of low levels of

<sup>®</sup> Abstract published in *Advance ACS Abstracts*, March 15, 1997.

(1) (a) Liu, C.-Y.; Pan, H.-L.; Fox, M. A.; Bard, A. J. *Science* **1993**, *261*, 897. (b) Liu, C.-Y.; Pan, H.-L.; Bard, A. J.; Fox, M. A. U.S. Patent 5,327,373, 1995. (c) Liu, C.-Y.; Hasty, T.; Bard, A. J. *J. Electrochem. Soc.* **1996**, *143*, 1914. (d) Liu, C.-Y.; Pan, H.-L.; Fox, M. A.; Bard, A. J., submitted. (e) Liu, C.-Y.; Tang, H.; Bard, A. J. *J. Phys. Chem.* **1996**, *100*, 3587. (f) Liu, C.-Y.; Pan, H.-L.; Tang, H.; Fox, M. A.; Bard, A. J. *J. Phys. Chem.* **1995**, *99*, 7632.

(2) (a) Gregg, B. A.; Fox, M. A.; Bard, A. J. *J. Am. Chem. Soc.* **1989**, *111*, 3024. (b) Gregg, B. A.; Fox, M. A.; Bard, A. J. *J. Phys. Chem.* **1990**, *94*, 1586. (c) Gregg, B. A.; Fox, M. A.; Bard, A. J. *J. Phys. Chem.* **1989**, *93*, 4227.

(3) (a) Simon, J.; Bassoul, P. In *Phthalocyanines, Properties and Applications*; Leznoff, C. C., Lever, A. B. P., Eds.; VCH: New York, 1989; Vol. 2, p 223. (b) Simon, J. In *Nanostructures Based on Molecular Materials*; Gopel, W., Ziegler, Ch., Eds.; VCH: Weinheim, 1992; p 267 and references therein.

(4) (a) Boden, N.; Bushby, R. J.; Clements, J. *J. Chem. Phys.* **1993**, *98*, 5920. (b) Boden, N.; Borner, R. C.; Bushby, R. J.; Clements, J. *J. Am. Chem. Soc.* **1994**, *116*, 10807.

(5) Wright, J. D. *Molecular Crystals*, 2nd ed.; Cambridge University Press: Cambridge, 1995.

(6) Gregory, P. *High-Technology Applications of Organic Colorants*; Plenum Press: New York, 1991.

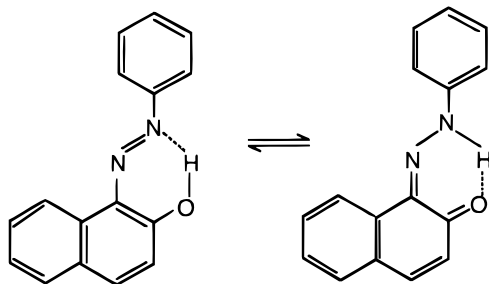
(7) Forrest, S. R. *IEEE Circuits and Devices Magazine*, May 1989, p 33.

(8) (a) Chandrasekhar, S.; Sadashiva, B. K.; Suresh, K. A. *Pramana* **1977**, *9*, 471. (b) Goodby, J. W.; Robinson, P. S.; Teo, B.-K.; Clad, P. E. *Mol. Cryst. Liq. Cryst. Lett.* **1980**, *56*, 303. (c) Morelli, G.; Ricciardi, G.; Roviello, A. *Chem. Phys. Lett.* **1991**, *185*, 468.

(9) Silinsh, E. A.; Capek, V. *Organic Molecular Crystals: Interaction, Localization, and Transport Phenomena*; American Institute of Physics: New York, 1994.

impurities (dopants) on the properties. Thus, as with inorganic semiconductors, the intrinsic features of the conductance in a substance can be obtained only by investigation of high-quality single crystals.

One of the most striking features of many organic crystals is that the low symmetry of molecules can induce lattice anisotropy and a corresponding anisotropy in the optical, electrical, and mechanical properties of the crystal. Such highly anisotropic molecular systems may be important in the development of molecular devices.<sup>5,9</sup> Unfortunately, this important characteristic of organic molecular crystals could not be probed in the early studies with randomly oriented polycrystalline samples, where a one-dimensional electronic material could not be distinguished from a three-dimensional one. The crystal orientation relative to a contacted electrode surface has a strong influence on its optoelectronic properties.<sup>1e,f</sup> It is therefore useful to develop a method for the manipulation of crystal orientation to characterize the inherent conductivity of the organic materials and to optimize these in potential applications. Here we show the possibility of controlling the orientation of quasi-1D single crystals of 1-(phenylazo)-2-naphthol (Sudan I) in ITO sandwich cells through the application of an electric field during crystal growth. An enhancement of the short-circuit photocurrent by 14 times is demonstrated. An electric field has been previously employed for aligning organic molecules in liquid crystal displays,<sup>10</sup> for poling of polymers in nonlinear optical systems,<sup>11,12</sup> and for generating anisotropic behavior in electrooptics.<sup>13</sup> However, the work reported here is the first to influence optoelectronic properties by manipulating crystal growth with an electric field.



The crystal structure of Sudan I was reported several years ago in two independent studies.<sup>14,15</sup> The results were consistent and were reported for data taken at three different temperatures. A C-centered monoclinic structure for a planar molecule with an intramolecular N—H...O hydrogen bond was reported.<sup>15</sup> The early studies focused primarily on the tautomeric equilibrium involving intramolecular proton transfer between N and O atoms in the solid, but the relationship between the molecular arrangement and the crystal morphology has not been reported. Since this relationship is essential to the understanding of the electrical properties of the

**Table 1. Crystallographic Data for C<sub>16</sub>H<sub>12</sub>N<sub>2</sub>O<sup>a</sup>**

formula	C <sub>16</sub> H <sub>12</sub> N <sub>2</sub> O	$\rho_{\text{calc}}$ , g/cm <sup>3</sup>	1.33
fw	248.28	reflections	12 183
		measured	
a, Å	5.8225(15)	unique reflections	5723
b, Å	17.377(5)	decay correction	0.975–1.01
c, Å	24.598(5)	$R_{\text{int}}$ ( $F^2$ )	0.196
$\beta$ , deg	92.37(2)	$\mu$ , cm <sup>-1</sup>	0.85
V, Å <sup>3</sup>	2486.7(11)	crystal size, mm	0.05 × 0.14 × 0.83
Z	8	transmission	N/A
		factor range	
F(000)	1040	$R_w(F^2)^b$	0.2597
crystal system	monoclinic	$R(F)^c$	0.0958
space group	$P2_1/c$	goodness of fit, $S^d$	0.984
T, °C	-100	parameters	344
2 $\theta$ range, deg	4–55	max $ \Delta/\sigma $	<0.1
scan speed (°/min)	6–15	min, max peaks	-0.23, 0.69
		(e <sup>-</sup> /Å <sup>3</sup> )	

<sup>a</sup> Data were collected on a Siemens P4 diffractometer equipped with a Nicolet LT-2 low-temperature device and using graphite monochromatized Mo K $\alpha$  radiation ( $\lambda = 0.71073$  Å). Data were collected using  $\omega$  scans with a scan range of 1° in  $\omega$ . Lattice parameters were obtained from the least-squares refinement of 50 reflections with  $9.8 < 2\theta < 19.2^\circ$ . <sup>b</sup>  $R_w = \{\sum w(|F_o|^2 - |F_c|^2)^2 / \sum w(|F_o|^4)^{1/2}\}$ , where the weight,  $w$ , is defined as  $w = 1/[\sigma^2(|F_o|^2) + (0.0728P)^2]$ ;  $P = [1/3(\text{maximum of } (0 \text{ or } |F_o|^2) + 2/3|F_c|^2)]$ . <sup>c</sup> The conventional  $R$  index based on  $F$  where the 1728 observed reflections have  $F_o > 4(\sigma(F_o))$ . <sup>d</sup>  $S = [\sum w(|F_o|^2 - |F_c|^2)^2 / (n - p)]^{1/2}$ , where  $n$  is the number of reflections and  $p$  is the number of refined parameters.

Sudan I crystal and the interpretation of the experimental results, we completed a crystal structure analysis in this study. We found that crystals grown from acetone were of a different crystalline form than those previously reported.

## Experimental Section

**Single-Crystal Growth.** Sudan I (~97%) was purchased from Aldrich and was further purified by sublimation within a 1-m-long glass tube with a temperature gradient from 100 to 25 °C. Crystals were grown from saturated acetone solution in Pyrex round-bottom tubes which were left undisturbed for the duration of the crystallization process. The tubes were covered with tissue paper and the solvent was allowed to evaporate slowly from the solution at room temperature. In another approach, solvent with a slight excess of solid was heated to 80 °C so that all the Sudan I solid was completely dissolved in the acetone. The hot concentrated solution was then slowly cooled to room temperature and left undisturbed for crystallization to occur over 1 day.

In all the cases, crystals grown from the solution were needle-shaped about 10–30 mm long and 0.1–0.3 mm across. The length of crystal needles was close to the depth of the solution used for crystal growth. These crystals were used for X-ray diffraction studies and some of the electrical characterization. Needle crystals were also obtained by solidification of the melt in ITO symmetric sandwich cells, as described below. Detailed procedures for the cell fabrication and filling were reported previously.<sup>1f,2b</sup>

**X-ray Diffraction.** The data were collected at 173 K on a Siemens P4 diffractometer equipped with a Nicolet LT-2 low-temperature device and using a graphite monochromator with Mo K $\alpha$  radiation ( $\lambda = 0.71073$  Å). Details of crystal data, data collection, and structure refinement are listed in Table 1. Three reflections (-1,2,5; -1,0,-6; 1,-1,5) were remeasured every 97 reflections to monitor instrument and crystal stability. A smoothed curve of the intensities of these check reflections was used to scale the data. The scaling factor ranged from 0.975 to 1.01. The data were corrected for Lp effects but not absorption. Data reduction and decay correction were performed using the SHELXTL/PC software package.<sup>16</sup> The structure was solved by direct methods and refined by full-matrix least-squares<sup>16</sup> on  $F^2$  with anisotropic thermal parameters for the non-H atoms. The hydrogen atoms were calculated in idealized positions (N—H 0.90 Å, C—H 0.96 Å) with isotropic temperature factors set to 1.2  $U_{\text{eq}}$  of the attached

(10) Castellano, J. A. *Handbook of Display Technology*; Academic Press: San Diego, 1992.

(11) *Nonlinear Optical Properties of Organic Molecules and Crystals*; Chemla, D. S., Zyss, J., Eds.; Academic Press: Orlando, 1987; Vol. 1.

(12) Williams, D. J. *Angew. Chem., Int. Ed. Engl.* **1984**, *23*, 690–703.

(13) *Molecular Electrooptics*; O'Konski, C. T., Ed.; Marcel Dekker: New York, 1976.

(14) Salmen, R.; Malterud, K. E.; Pedersen, B. F. *Acta Chem. Scand.* **1988**, *42*, 493.

(15) Olivieri, A. C.; Wilson, R. B.; Paul, I. C.; Curtin, D. Y. *J. Am. Chem. Soc.* **1989**, *111*, 5525.

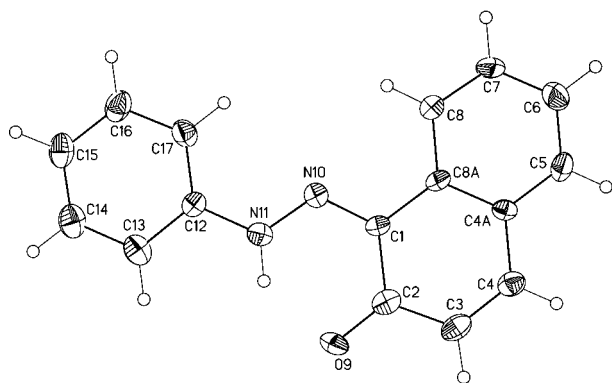


**Figure 1.** Thermal ellipsoid representation of  $C_{16}H_{12}N_2O$  (**1**) showing the atom labeling scheme. The labeling scheme for **2** is identical with atom labels appended by 'a'. The thermal ellipsoids are scaled to the 30% probability level. Hydrogen atoms are drawn to an arbitrary scale.

atom. The function  $\sum w(|F_o|^2 - |F_c|^2)^2$ , was minimized, where  $w = 1/[(\sigma(F_o))^2 + (0.0728P)^2]$  and  $P = (|F_o|^2 + 2|F_c|^2)/3$ . The data were corrected for secondary extinction effects. The correction takes the form  $F_{corr} = kF_o/[1 + 4(1 \times 10^{-6}F_c^2\lambda^3/\sin(2\theta))]^{0.25}$  where  $k$  is the overall scale factor. Neutral atom scattering factors and values used to calculate the linear absorption coefficient are from the *International Tables for X-ray Crystallography*.<sup>17</sup> Other computer programs used in this work are listed elsewhere.<sup>18</sup> All figures were generated using SHELXTL/PC.<sup>16</sup>

**Conductivity Measurement.** Because crystals of Sudan I are highly resistive, conductivity measurements can be compromised by leakage currents on the substrate holding the crystals (e.g., glass) and by the finite input impedance of the measuring device. In our studies, Teflon was used as the sample holder. Connection to the crystals was made with two Pt-on-glass slides or ITO glass pieces which were placed alongside each other (with 80- $\mu$ m separation) on the Teflon holder by manipulation under an optical microscope. The Pt had been sputtered on the glass slides to make a good contact with the crystal needles, which were laid on top of the Pt films and attached to the Pt with Ga-In alloy. A home-built high-sensitivity ( $\sim$ pA) amplifier and PAR universal programmer (Model 175) were used to obtain  $I$ - $V$  curves. Measurements with a single-crystal needle were not successful, because the current was too small to be detected, even with a crystal length of about 80  $\mu$ m. Thus, to increase the contact area, several hundred crystal needles arranged parallel to each other were used. These crystal needles did not overlap each other and could be seen individually. The cross section of each needle was determined microscopically from its diameter. The total number of needles was taken to yield a total cross section for the calculation of conductivity along the needle direction. The measurements of current perpendicularly across the needles were carried out with ITO/Sudan I/ITO sandwich cells. In this case, the thickness of the thin film was used as the length for the calculation. For the photocurrent experiments, ITO/Sudan I/ITO cells were irradiated with a 20 W tungsten lamp through an optical fiber.

## Results and Discussion

**X-ray Diffraction Data.** Details of crystallographic data and structure refinement for the red, needle-shaped Sudan I single crystals are given in Table 1, and the bond lengths and angles are listed in Table 2. A thermal ellipsoid representation for this molecule with the atom-labeling scheme is shown in Figure 1. The

**Table 2. Bond Lengths ( $\text{\AA}$ ) and Angles (deg) for the Non-hydrogen Atoms of  $C_{16}H_{12}N_2O$**

			1		2	
1	2	3	1-2	1-2-3	1-2	1-2-3
C2	C1	C8A	1.473(9)	120.3(5)	1.458(9)	119.5(5)
C8A	C1	N10	1.446(9)	116.9(5)	1.451(9)	115.8(5)
N10	C1	C2	1.322(8)	122.8(6)	1.330(8)	124.6(6)
C3	C2	O9	1.436(9)	122.0(6)	1.430(9)	122.0(6)
C3	C2	C1		116.5(6)		117.3(6)
O9	C2	C1	1.273(9)	121.5(6)	1.266(8)	120.7(5)
C4	C3	C2	1.356(10)	122.1(7)	1.337(9)	122.5(6)
C4A	C4	C3	1.433(9)	122.3(6)	1.459(9)	121.9(6)
C5	C4A	C8A	1.393(10)	119.7(6)	1.382(9)	120.2(6)
C5	C4A	C4		121.2(6)		121.5(6)
C8A	C4A	C4	1.408(8)	119.1(6)	1.399(9)	118.2(6)
C6	C5	C4A	1.368(10)	120.9(6)	1.374(10)	120.9(6)
C7	C6	C5	1.380(10)	118.7(7)	1.382(10)	119.4(7)
C8	C7	C6	1.361(10)	122.9(7)	1.368(10)	121.5(6)
C8A	C8	C7	1.410(9)	118.9(6)	1.425(9)	119.5(6)
C1	C8A	C4A		119.6(5)		120.4(6)
C1	C8A	C8		121.6(5)		121.2(6)
C4A	C8A	C8		118.8(6)		118.3(6)
N11	N10	C1	1.314(8)	119.1(5)	1.300(7)	119.0(5)
C12	N11	N10	1.397(8)	121.0(5)	1.416(7)	119.4(5)
C13	C12	C17	1.399(10)	121.1(6)	1.388(9)	120.3(5)
C13	C12	N11		116.9(6)		118.4(6)
C17	C12	N11	1.383(9)	122.0(6)	1.387(9)	121.3(6)
C14	C13	C12	1.383(10)	117.3(6)	1.375(9)	120.1(6)
C15	C14	C13	1.381(11)	122.5(7)	1.385(10)	119.4(6)
C16	C15	C14	1.385(12)	119.2(7)	1.378(10)	120.2(6)
C17	C16	C15	1.387(10)	119.9(7)	1.367(9)	120.9(6)
C12	C17	C16		120.0(7)		119.1(6)

structure reported here is for a second crystallographic form known for this compound.<sup>14,15</sup> Olivieri et al.<sup>15</sup> reported a monoclinic C-centered cell of dimensions:  $a = 27.875(7)$ ,  $b = 6.028(2)$ ,  $c = 14.928(5)$   $\text{\AA}$ ,  $\beta = 103.57(2)^\circ$ ,  $V = 2434(3)$   $\text{\AA}^3$ ,  $Z = 8$ ,  $\rho = 1.36$   $\text{g cm}^{-3}$  at 213 K for a molecule of formula  $C_{16}H_{12}N_2O$ . This polymorphic form has a slightly higher density,  $\rho = 1.36$   $\text{g cm}^{-3}$ , than that observed for the form we report here,  $\rho = 1.33$   $\text{g cm}^{-3}$ . We did not obtain the C-centered polymorph by our crystallization methods. The structure of Sudan I was discussed in depth in the earlier reports,<sup>14,15</sup> and our results (Figure 2) are consistent with the molecular geometrical features reported. The geometry of the molecules in the two environments (designated **1** and **2**) reported here is essentially the same, as is generally the case in crystal structures containing symmetry-independent molecules.<sup>19,20</sup> The molecules are planar having average deviations from the mean molecular plane of less than 0.05  $\text{\AA}$  with a maximum deviation of 0.115  $\text{\AA}$  for O9 of **1**. The previous work on Sudan I focused on the azo/hydrazo tautomeric equilibrium possible for such materials.<sup>14,15</sup> The molecule more closely resembles the hydrazo form with a carbonyl type oxygen ( $C-O_{\text{avg}} 1.270(6)$   $\text{\AA}$ ), an exocyclic C-N double bond ( $C-N_{\text{avg}} 1.326(6)$   $\text{\AA}$ ) and a localized C-C double bond between C3 and C4 ( $C-C_{\text{avg}} 1.346(7)$   $\text{\AA}$ ) and appears to have an intramolecular hydrogen bond between the hydrazo nitrogen, N11, and the carbonyl oxygen, O9. Using idealized hydrogen atom coordinates, the geometry of these interactions are  $N11-H11 \cdots O9$ ,  $N \cdots O 2.532(7)$   $\text{\AA}$ ,  $H \cdots O 1.803(7)$   $\text{\AA}$ ,  $N-H \cdots O 136.5(6)^\circ$ , and  $N11'-H11' \cdots O9'$ ,  $N \cdots O 2.564(6)$   $\text{\AA}$ ,  $H \cdots O 1.853(6)$   $\text{\AA}$ , and  $N-H \cdots O 134.3(6)^\circ$ . The close  $\pi$ - $\pi$  stacking observed for the C-centered polymorph is retained here as well. The molecules stack along the short **a** axis in our polymorphic form, while in the

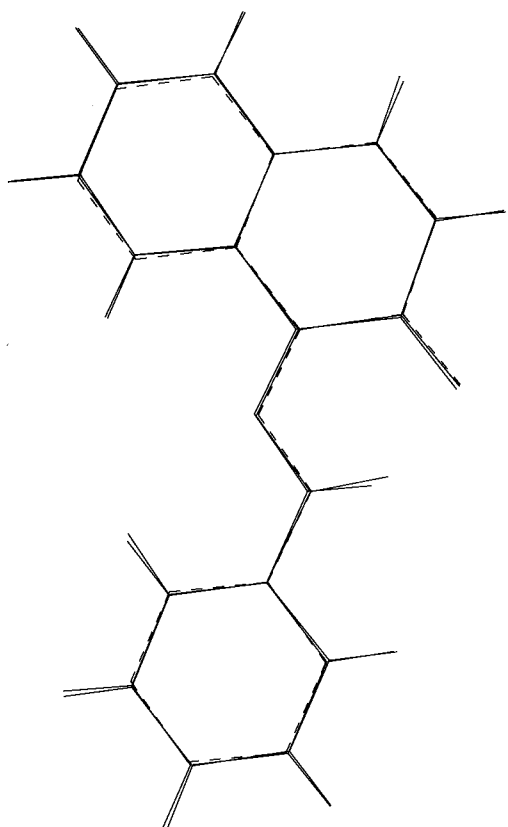
(16) Sheldrick, G. M. SHELXTL/PC (Version 5.03); Siemens Analytical X-ray Instruments, Inc.: Madison, WI, 1994.

(17) *International Tables for X-ray Crystallography*; Wilson, A. J. C., Ed.; Kluwer Academic Press: Boston, 1992; Vol. C, Tables 4.2.6.8 and 6.1.1.4.

(18) Gadol, S. M.; Davis, R. E. *Organometallics* **1982**, *1*, 1607.

(19) Gautham, N. *Acta Crystallogr.* **1992**, *B48*, 337.

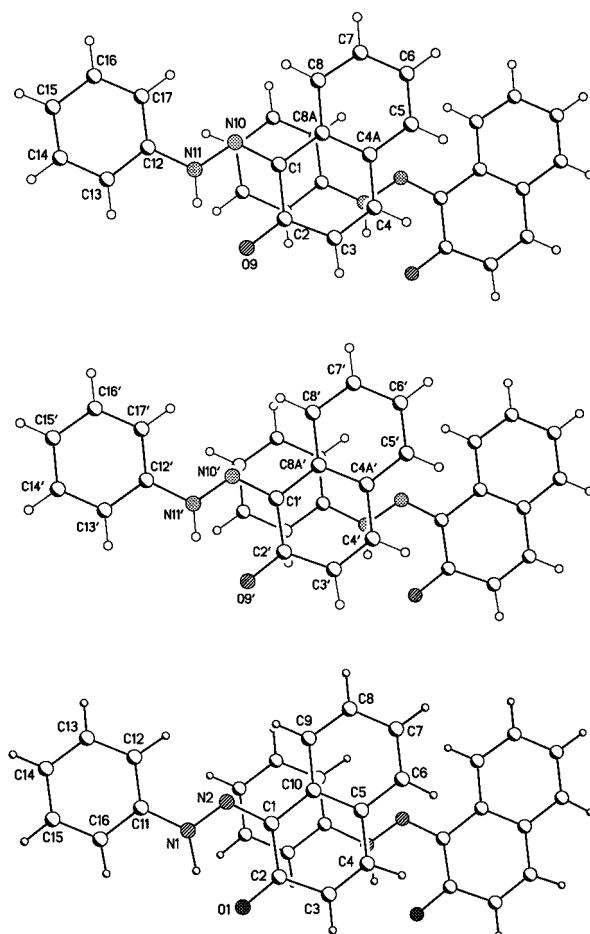
(20) Sona, V.; Gautham, N. *Acta Crystallogr.* **1992**, *B48*, 111.



**Figure 2.** Illustration of the nearly identical geometry of the two unique molecules of  $C_{16}H_{12}N_2O$  and of the C-centered polymorph. The figure was obtained by fitting **1** onto the equivalent non-hydrogen atoms of **2**. These molecules are shown with solid lines and have hydrogen atoms included. Atoms of the 213 K structure of the C-centered polymorph (dashed lines) were then fitted to the equivalent atoms of **2**.

C-centered polymorph, molecules stack along the **b** axis. The closest intermolecular contacts are between molecules related by an **a**-axis translation. Adjacent molecules are offset so that a carbon atom bound to a nitrogen atom is approximately centered over an aromatic ring in the molecule above (or below; Figure 3). This mode of stacking is observed for our structure and for the C-centered modification as well. The packing results in columns of  $\pi$ -stacked molecules extending along **a**; i.e., the crystals grew as very long thin needles extended along the (100) direction. The plane-to-plane separation is 3.34 Å for **1** and 3.24 Å for **2** (Figure 4). A value of 3.34 Å was observed for the C-centered morphology at 213 K.<sup>15</sup> The molecules are tilted by 34.9° and 33.9° for **1** and **2**, respectively, with respect to the **a** axis. In the C-centered modification, the molecules are tilted by 33.6° with respect to the **b** axis. The difference in the molecular packing between the two polymorphs is in how the columns of  $\pi$ -stacked molecules are arranged. In our structure, columns of  $\pi$ -stacked molecules are surrounded by six columns of neighboring molecules. In the C-centered polymorph, each column of  $\pi$ -stacked molecules is adjacent to eight other columns of molecules (Figure 5).

**Electrical Characterization.** Needle-shaped single crystals of Sudan I were formed upon capillary-filling from its molten state ( $\sim 133$  °C) into cells constructed with two parallel pieces of ITO-coated glass followed by slow cooling to room temperature. All the cells with thicknesses of 2–10  $\mu\text{m}$  produced similar crystals. The cross section of these needle-shaped crystals varied from



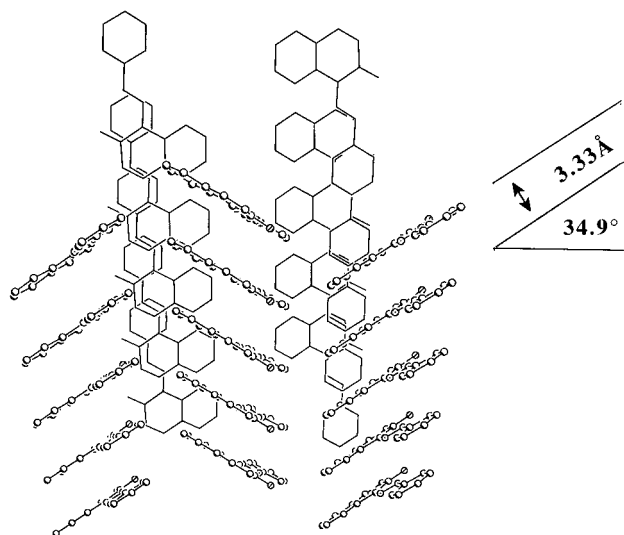


**Figure 4.** Unit-cell packing diagram for  $C_{16}H_{12}N_2O$ . **1** is shown as a ball-and-stick figure, and **2** is represented as a wire-frame drawing. The view direction is parallel to the plane through **1** and is nearly perpendicular to the plane through atoms of **2**. The perpendicular distance between  $\pi$ -stacked **1** is shown. This value is 3.24 Å for **2** and 3.34 Å for the C-centered polymorph. The essentially planar molecules are similarly inclined with respect to the stacking axis. The angle for **1** is shown and is close to the 33.9° observed for **2** and the 33.6° for molecules of the C-centered polymorph.

The parallel resistivity (along the needle axis of the quasi-1D molecular crystal),  $\rho_{\parallel}$ , was determined from isolated Sudan I single-crystal needles prepared from a saturated acetone solution. The individual crystal needles grown from the solution were actually a bundle of even thinner crystal needles or fibers lying parallel to each other that could be easily separated without breaking. The elementary component of the crystal needle is believed to be the individual molecular column as indicated by the X-ray diffraction results. These molecular columns were held together by weak van der Waals forces which were responsible for the high resistivity ( $\rho_{\perp}$ ). In contrast, the intermolecular interaction along the crystal needle was much stronger; it was harder to break the crystal than to separate the needles, as suggested by the X-ray diffraction structure. Figures 3 and 4 show that the planar molecules stacked one above another in parallel and that they lined up in regular molecular columns along the needle axis. The better intermolecular  $\pi$ - $\pi$  overlap made the crystal mechanically stronger along the needle axis. This structure also suggests that the molecular columns should show a lower  $\rho_{\parallel}$  than  $\rho_{\perp}$ .  $\rho_{\parallel}$ , measured with needles oriented across two contacts, was on the order of  $10^{14}$ , more than 2 orders of magnitude lower than  $\rho_{\perp}$ , as calculated from the  $i$ - $V$  curve shown in Figure 8. Note that in such measurements, the background level (i.e., in the absence of Sudan I crystal) was flat over the entire potential range used, and no leakage current was observed. This is important to ensure the accuracy of the measurements. On the other hand, the cross section of some single-crystal needles employed were irregular and could not be precisely determined. This necessarily gave rise to variations in the calculated contact area and therefore the resistivity. However, the error was no more than  $\pm 20\%$ . Because  $\rho_{\parallel}$  was measured between two Pt electrodes and  $\rho_{\perp}$  between two ITO electrodes, the contact resistance may play a role. However, we found that both Pt and ITO-coated glass

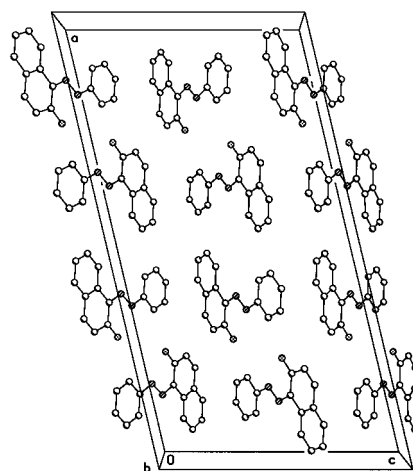
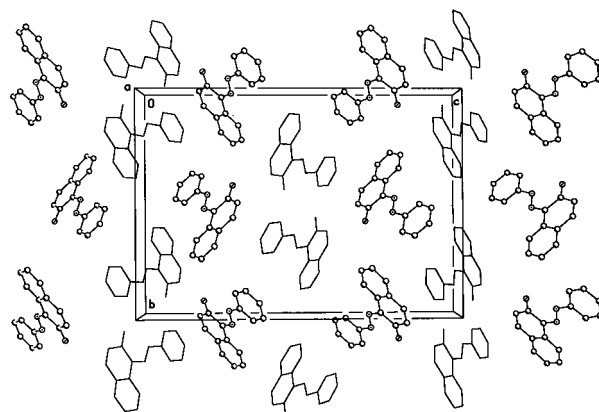


**Figure 5.** Single layer perpendicular to the short crystallographic axis shown for the two polymorphic forms of Sudan I illustrating the different modes of packing of the columns of  $\pi$ -stacked molecules in the two forms. In the primitive monoclinic form, each column of molecules is adjacent to six columns of neighboring molecules. In the C-centered polymorph, there are eight adjacent stacks of molecules.

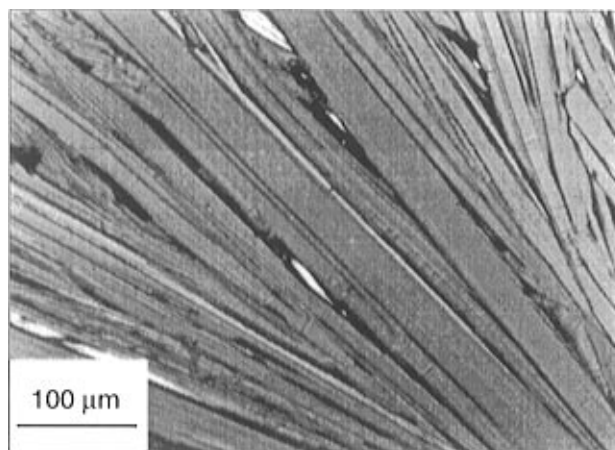


**Figure 6.** Micrograph of Sudan I single crystals between two pieces of ITO-coated glass ( $\sim 5 \mu\text{m}$  thick).

in connection with Sudan I crystals yielded conductivities of the same order of magnitude in measurements of current along the needles. Moreover, the polymorph of Sudan I single-crystal needles grown from the melt in ITO cells matched one grown from solution, as described above, and did not match the one reported earlier,<sup>14,15</sup> as verified again with X-ray diffraction measurements. Individual Sudan I needles grown from the melt were too thin for single-crystal X-ray diffrac-

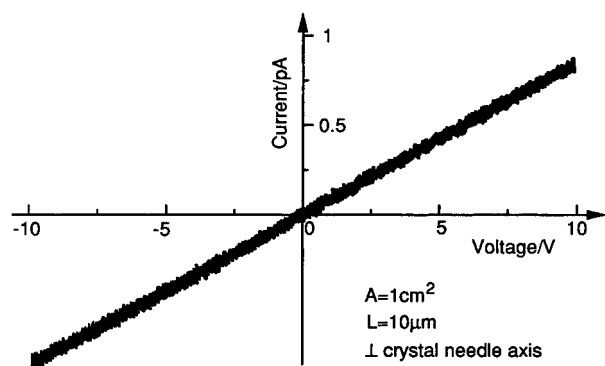


**Figure 7.** Current as a function of bias voltage applied perpendicular to the crystal needle axis of 1-(phenylazo)-2-naphthol.

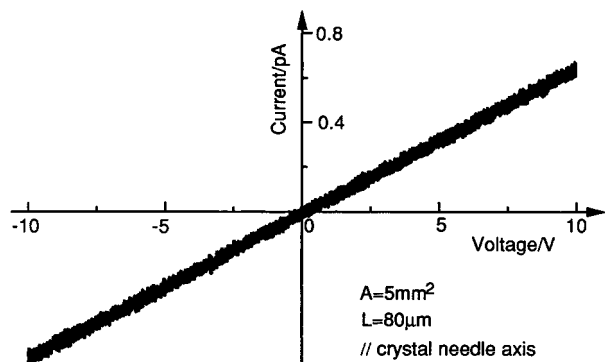


**Figure 8.** Current as a function of bias voltage applied parallel to the crystal needle axis of 1-(phenylazo)-2-naphthol. The quoted area represents an estimate of the sum of the cross-sectional areas of the needles.

tion. A large number of single-crystal needles were scraped from the ITO substrates and subjected to X-ray powder pattern characterization. Comparison of these results with simulations for the two structurally different crystals grown from the solutions show that the Sudan I single-crystal needles grown from both solution and melt have the same crystal structure (see Supporting Information). Therefore, the conductivity results ( $\rho_{\parallel}$  and  $\rho_{\perp}$ ) are comparable.

Such an anisotropy of conductivity confirms a direction-dependent carrier-transport rate in Sudan I single crystals. The stronger interaction between the orbitals of neighboring molecules within the same column lowered the potential barriers and thus enhanced the intermolecular electron transfer or hopping. Knowledge of the relationship between the arrangement of the individual molecules and their electronic properties is important in the design of devices based on molecular crystals, allowing the assembly of molecules in a structure to obtain a desired electronic behavior.

**Effect of Electric Field on Crystal Growth.** The growth mechanism of most organic molecular crystals on a substrate is usually not well-defined, even when carried out by a controlled epitaxial technique.<sup>21</sup> However, lattice mismatch, i.e., the differences in size and angle between the unit-cell dimensions of the substrate and crystal, which is crucial for the growth of inorganic crystals, does not seem to be as important for the growth of organic molecular crystals.<sup>21</sup> Geometric properties of the molecules and interactions between an individual molecule and the substrate are believed to be controlling

factors.<sup>21</sup> Recent calculations show that it is the shallow potential wells which define the substrate–molecular layer interaction that allow molecules to sit on noncommensurate positions.<sup>22</sup> We thought that if the asymmetric structure and dipole moment<sup>23</sup> of the Sudan I molecule were important for the preferential orientation of the needle crystal parallel to the ITO surface, then the application of an electric field across the ITO/Sudan I/ITO cells should influence the orientation of the dipolar molecules in the melt, and thus, the direction of the crystal growth could be influenced in a way similar to the poling of polymers.<sup>11,12</sup> Indeed, when a bias of 1 V was applied between the two ITO electrodes during crystal growth, the resulting crystal was featureless and no needle structure was visible. This was confirmed using twin cells in which a narrow strip ( $\sim 2$  mm) of ITO film in the middle of each electrode was etched away with sulfuric acid so that each electrode would have two physically separate parts. The twin cells were placed in an oven at a temperature of 145–150 °C and were then filled by capillary action with Sudan I molecules. As the crystals grew through slow cooling of the filled cells to room temperature, only one-half of the twin cell was subjected to the bias voltage. Thus the conditions for crystal growth in these two-part cells were identical except for the electric field. The needlelike structures were seen only in the field-free sides of the cells. We believe that the crystal needle axis, which was parallel to the electrode in a field-free region, tilted to some degree against the ITO as a result of the electric field so that only the ends, rather than the whole bodies, of the needle crystals could be seen. We tried to verify the different orientations of the crystals grown in the electric field with infrared spectroscopy by monitoring the carbonyl band. In this experiment, the two pieces of ITO glass were separated after Sudan I crystals were grown in the sandwich cell with and without an electric field and IR reflectance measurements were carried out with a Magna-IR 550 spectrometer (Nicolet). Unfortunately, no IR signal was detectable from any of our Sudan I crystal thin films after over 1000 scans. Since the carbonyl group has a very large extinction coefficient, our Sudan I single crystal films were too thick for transmission IR spectroscopy.

**Photocurrent Measurements.** Measurements of short-circuit photocurrent ( $I_{sc}$ ) from ITO/Sudan I/ITO cells revealed that  $I_{sc}$  was about 14 times higher from cells prepared with an electric field than field-free cells (Figure 9). Due to better  $\pi$ – $\pi$  overlap along the needle,  $\rho_{\perp}$  is over 100 times higher than  $\rho_{\parallel}$ . Thus with the tilt of the needle axis at an angle to the ITO surface caused by the electric field during crystal growth, a higher conductivity and thus a higher current could be obtained in the ITO/Sudan I/ITO cells. This was confirmed by the measurement of dark and photo currents as a function of bias voltage (Figure 10). In both cases, the  $I$ – $V$  curves were straight lines, and the conductance of the cells was obtained from the slope of these lines. The conductance of the cells prepared with an electric field was about 8–9 times higher than those prepared without the field. This ratio was about the same for both photo and dark measurements, indicating that the

(21) Kobayashi, T. In *Organic Crystals I: Characterization*; Karl, N., Ed.; Springer-Verlag: Berlin, 1991; pp 1–63.

(22) Hillier, A. C.; Ward, M. D. *Phys. Rev. B* **1996**, *54*, 14037.

(23) Bishai, A. M.; Shakra, S.; Hakim, I. K. *Polym. Photochem.* **1982**, *2*, 269–275.

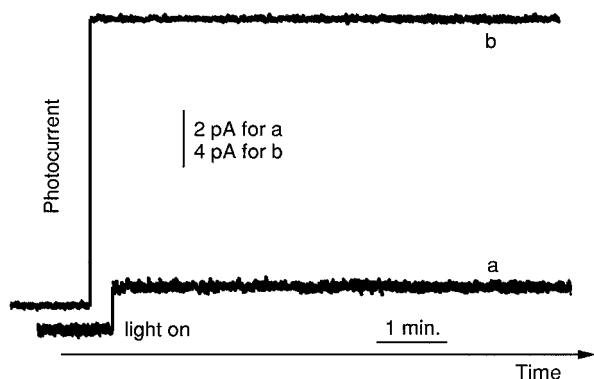


**Figure 9.** Short-circuit photocurrent as a function of time. ITO/Sudan I/ITO cells ( $\sim 5 \mu\text{m}$  thick,  $0.5 \text{ cm}^2$  area) were prepared (a) without and (b) with an electric field ( $\sim 2000 \text{ V/cm}$ ). The cell was irradiated with a 20 W tungsten lamp through and optical fiber. (Baseline of b shifted for clarity.)

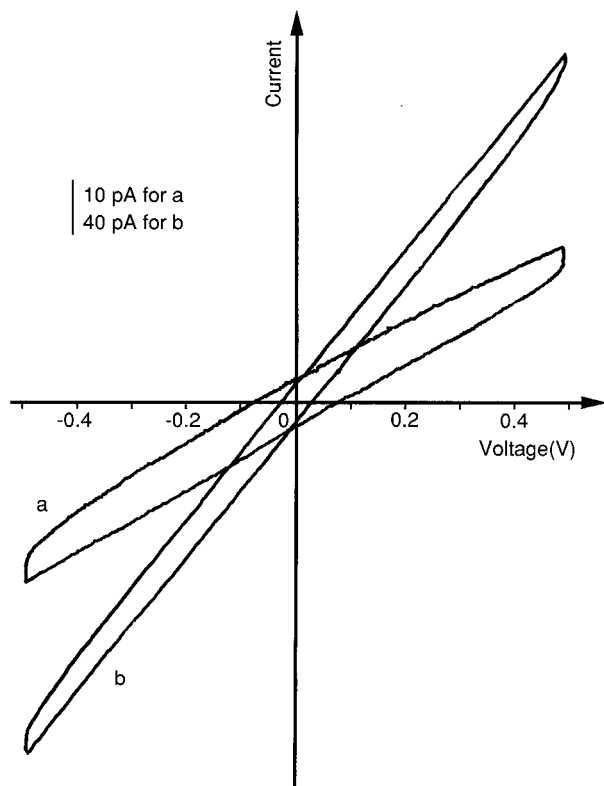


**Figure 10.** Photocurrent as a function of bias voltage for ITO/Sudan I/ITO cells prepared (a) without and (b) with an electric field. (Cell parameters and conditions as in Figure 9.)

intrinsic conductivity of the cells was indeed increased as a result of the electric-field-induced reorientation of the crystal needles. The photocurrent was about 26 times higher than the dark current at a given bias, because irradiation induced a population increase in the charge carriers even with a weak light source.

Since  $\rho_{\perp}/\rho_{\parallel} > 100$ , one would expect a current increase by more than 2 orders of magnitude if the crystal needles reoriented themselves from parallel to perpendicular to the ITO electrode. If the electric field was able to align the dipolar molecules to highest degree possible ( $90^\circ$ ), i.e., if the molecular plane was parallel to the electric field with no thermal disturbances, the crystal needles would be tilted less than  $55^\circ$  against the electrode plane. X-ray diffraction of the Sudan I crystal needles shows that the molecular plane is tilted  $34.9^\circ$  relative to the needle axis. Thus the photocurrent under bias was increased by only 8–9 times.

The short-circuit photocurrent is produced by a preferential photoinjection of electrons from the excited Sudan I molecules into the irradiated ITO electrode and holes into the organic layer followed by charge carrier transport through the whole film, as discussed previously for ITO/porphyrin/ITO cells.<sup>2b</sup> Thus,  $I_{sc}$  is controlled by two factors, interfacial charge separation and charge carrier transport. The larger enhancement in short-circuit photocurrent (14 times) than in photocurrent under bias (8–9 times) indicates that the reorientation of the Sudan I crystal needle not only increased the conductivity of the cell but also improved the interfacial separation. This effect may be of use in the fabrication of organic optoelectronic devices.

## Conclusions

The results reported here show a correspondence between crystal structure morphology and electrical properties. The perpendicular distance between neighboring molecules within the same column is about  $3.34 \text{ \AA}$ , as shown in Figure 4, and the intermolecular separation along the column axes is even larger ( $4.18 \text{ \AA}$ ). These structural features suggest that the Sudan I single crystal is a highly insulating material, even along the needle axis, which is consistent with our experimental resistivities. Upon irradiation, however, the resistivity decreased by several orders of magnitude, depending on the light intensity, and a steady-state short-circuit photocurrent was generated from ITO/Sudan I/ITO symmetrical sandwich cells. Such photoconductive insulators are very promising materials for high-density data storage.<sup>1a–d</sup> In this case, irradiation induces charge trapping and detrapping, which represent the writing and reading processes, respectively. Data are stored in the form of charge. Therefore, the dark insulating property of the memory media is important for long charge retention times. Organic materials which are among the most widely used electrical insulators have a potential for this kind of information storage. The crystal orientation of Sudan I can be manipulated by the application of an electric field during crystal growth, and the optoelectronic properties of ITO/Sudan I/ITO sandwich cells have been substantially improved as a result of this electric-field-induced reorientation. Such a field effect may be useful in the optimization of optoelectronic properties of molecular crystal-based devices.

**Acknowledgment.** We thank Dr. J. S. Swinnea for the X-ray powder diffraction measurements and Dr. F.-R. F. Fan for valuable discussions. The support of this research by grants from the National Science Foundation (CHE9423874) is gratefully acknowledged.

**Supporting Information Available:** Details of the powder diffraction experiments and tables of positional and thermal parameters, bond lengths, angles and torsion angles, and thermal ellipsoid and unit cell diagrams (21 pages). Ordering information is given on any current masthead page.